Final synopsis of the thesis entitled

Development of nanoparticle based biomolecule probes for detection and management of diseases

Submitted by

Shripriya Kishanlal Purohit

In Fulfillment of Requirement for the Award of

Doctor of Philosophy

In the faculty of Science and Technology
(Biosciences)
Mangalore University

Research Supervisor

Dr. Vijay B. Kadwad

Scientific Officer & Dy General Manager, TCK & RIA
and In-Charge, BRIT Regional Centres, Delhi, Hyderabad & Bengaluru

---

Board of Radiation and Isotope Technology (BRIT)
BARC Vashi Complex, Sector 20

Vashi, Navi Mumbai, 400 703

June 2022

1. Introduction and review of literature

Nanotechnology is emerging as a promising approach for in-vivo and in-vitro medical and biological applications. In general, nanotechnology uses materials sized between 1 - 200 nm, often materials around micron size are also being used (Hong H *et al.*, 2009). The interdisciplinary nature of nanotechnology has exerted enormous influence in various fields, especially in medical science. Nanomedicine can be defined as the use of nanoparticles for detection, diagnosis, monitoring of physical and pathological processes for therapy and for control of biological systems (Anna L *et al.*, 2010, Debnath, B. *et al.,* 2009, Majid, A. *et al.,* 2011). "Nanoparticles are the particles with one or more dimensions at the nanoscale." General definition of the nanoscale is dimensions of the order of 200 nm or less. However, very often, besides "strictly nano (1-100 nm)" all submicron colloidal particles (1 – 1000 nm) are also referred as nanoparticles (Leary *et al.*, 2005, Gelperina *et al*., 2005). The classes of nanoparticles currently used in biotechnology and particularly in nanomedicine include liposomes, fullerenes, liquid crystals, quantum dots and superparamagnetic nanoparticles. Over the past two decades, superparamagnetic iron oxide nanoparticles have received enormous attention for diagnostic and therapeutic applications.

Nanoparticle based biomedical probes: In general, nanoparticles based biomedical probes have four main components: the core, the coating, the targeting biomolecule and a label. The coating is necessary for the introduction of linker groups, chelation sites and for the colloidal stability. If it is used for the in-vivo applications, coating is required for the biocompatibility, reduced uptake by the reticuloendothelial system (RES) and to avoid the premature clearance from the blood. Label can be a radioisotope, an enzyme or fluorescent / chemilumeniscent molecules which can be used for the final readout. Targeting biomolecules may be an antibody, various antigens expressed during the diseases, endocrine hormones, vitamins, drugs etc. Nanoparticles designed with linker groups or chelating sites on their surface can be conjugated with target specific biomolecules along with a suitable label for the detection, diagnosis and management of diseases.

Magnetic nanoparticles: There are reports on magnetic nanoparticles being utilized in medicine as the drug carriers, as contrast agents in magnetic resonance imaging (MRI) and magnetic hyperthermia (Xu, H. *et al.*, 2011, Kudr, J. *et al.*, 2017, Unak, P. 2008, Alina, M.P. *et al*., 2013). Multifunctional magnetic nanoparticles are also reported for diagnosis as well

as for therapy (Kohler *et al.*, 2005). Magnetic nanoparticles can be divided into two categories based on their structural configuration: (1) a magnetic particle core (typically magnetite, Fe_3O_4, or maghemite, Fe_2O_3) coated with a biocompatible polymers such as oleic acid, polyethylene glycol (PEG), dextran, alginate etc.; and (2) a porous biocompatible polymer in which iron oxide nanoparticles are entrapped within the polymer matrix.

Magnetic nanoparticle based biomedical probes in nuclear medicine: Radiolabelled magnetic nanoparticles are also used in both, in-vivo and in-vitro forms of nuclear medicine. Nanoparticle labelled antibodies, antigens and other biomolecules in association with radioisotopes such as ^{99m}Tc, ^{125}I, ^{131}I, ^{188}Re, ^{186}Re, ^{90}Y and ^{111}In are currently being used both in-vivo and in-vitro forms for diagnostic and/or therapeutic applications (Fu, C.M., *et al.,* 2004, Pellico, J. *et al.,*2017).

Technetium-99m (^{99m}Tc) is one of the important radioisotopes used in about 80% of all nuclear medicine procedures worldwide. Because of its 140 keV gamma-ray emission, its convenient half-life of 6 hours, it is the radioisotope of choice for single photon emission computed tomography (SPECT). ^{99m}Tc is known as 'work horse' of nuclear medicine. Technetium exhibits variable oxidation states and can complex with a variety of ligands forming different complexes, many of which are found to concentrate in specific organs. A relatively convenient half-life (60 days) and a low energy emission of photons, make iodine-125 (^{125}I), a preferred isotope for radiation therapy (brachytherapy) to treat prostate cancer and brain tumours. ^{125}I is also a radioisotope of choice for radioimmunoassay (RIA) and immunoradiometric assay (IRMA). Majority of in-vivo applications of nanoparticle based probes are reported in nuclear medicine such as drug delivery via magnetic targeting, hyperthermia, multimodal imaging (SPECT-MRI or positron emission tomography (PET)-MRI) etc. whereas important in-vitro applications include RIA / IRMA for detection and diagnosis of diseases.

Scope of the work

The Radiopharmaceuticals Unit of the Board of Radiation and Isotope Technology (BRIT) of Department of Atomic Energy (DAE), where this work was carried out, is involved in the R&D, production and supply of ^{99m}Tc based radiopharmaceuticals for the diagnosis of diseases in a number of tissue and organ systems, including bones, brain, heart, kidneys, liver, and lungs using SPECT. Apart from this, BRIT is also involved in

production and supply of RIA and IRMA kits for various hormones, including thyroid hormones, to various research centers and diagnostic laboratories throughout India.

Nowadays, the demand for hybrid imaging techniques is increasing dramatically. Multimodal or hybrid imaging systems are gaining importance and SPECT-CT is being widely used in India and abroad (Madru, R. *et al., 2012,* Tsoukalas, C. *et al.,* 2018*).* With recent unveiling of the hybrid SPECT-MRI (T. Sui, B. *et al.,* 2013*),* which has exceptional imaging capabilities, it has been necessary to develop physiologically stable multimodality imaging probes for SPECT-MRI using superparamagnetic iron oxide nanoparticles (SPION). SPECT-MRI will be reality in India soon. At present a limited number of multimodal imaging probes suitable for SPECT-MRI are reported in literature and being used in preclinical and potential clinical investigations (Yang, C.T. *et al.,* 2018, Misri, R. *et al.,* 2012*).*

In immunoassays based on magnetic particles, magnetic properties of the core is directly related to signal / noise (S/N) ratio or non-specific binding (NSB) thereby affecting the sensitivity of the assay. At present RIA kits supplied by BRIT are based on magnetizable cellulose particles (Kadwad V.B. *et al.,* 1996, Rasmi, R.R. *et al.,* 2014). Although magnetizable cellulose particles are good enough for immunoassays, still there is a scope for improving the magnetic responsiveness of regular magnetizable cellulose particles containing iron oxide core. Improved magnetic responsiveness of the magnetic core facilitates the efficient washing of magnetizable particles to reduce non-specific binding in immunoassay procedures. EP 93-113891 (31.8.93) reports an S/N ratio of the assay method using mixed crystal ferrite coated particles as 1.6 times greater than that of using conventional magnetite (iron oxide) coated particles. However, there are no reports on use of such mixed crystal ferrites with cellulose matrix. Hence, it will be logical, by replacing the iron oxide core of magnetizable cellulose by mixed crystal ferrite core, both the advantages associated with cellulose support matrix and magnetic core can be achieved.

Objectives

The present study will be taken up with a view to develop magnetizable nanoparticle based biomolecule probes suitable for detection and management of diseases including thyroid disorders with following objectives:

1. Development and evaluation of superparamagnetic nanoparticle based biomolecule probes by combining magnetic properties with radioisotopes for the potential use in in-vivo and in-vitro nuclear medicine applications.
2. Synthesis and characterization of versatile magnetizable nanoparticles of desired size, morphology, chemical composition and surface chemistry to be used as basic building blocks for architecture of biomolecule probe.
3. Functionalization of magnetizable nanoparticles with antibody and other biomolecules.
4. Optimization of radiolabelling procedures for magnetic nanoparticles with ^{99m}Tc and ^{125}I.
5. Development of magnetizable cellulose containing manganese ferrite core using synthesized magnetizable nanoparticles.
6. Application of magnetizable nanoparticles in comprehensive development of RIA procedures for thyroid hormones triiodothyronine (T3) and thyroxine (T4) followed by kit formulation for routine large scale production and supply.

The thesis is divided into 5 chapters:

Chapter 1: Introduction

Chapter 2: Preparation and characterization of magnetic nanoparticles

Chapter 3: Development of magnetic nanoparticle based biomolecule probes for use in nuclear medicine

Chapter 4: Summary and conclusions

Chapter 5: References

2 Preparation and characterization of magnetic nanoparticles

This chapter describes synthesis and evaluation of paramagnetic nanoparticles for their versatilities, possibilities and limitations for their applications in biomedicine, especially for use in nuclear medicine. Synthesis of two types of magnetizable nanoparticles is reported here: (1) superparamagnetic iron oxide nanoparticles (SPION) and (2) novel superparamagnetic iron oxide nanoparticles containing manganese ferrite core (Mn-SPION). It has been reported in the literature that magnetizable nanoparticles coated with oleic acid are highly biocompatible with reduced uptake by the reticuloendothelial system (RES) and

widely used in in-vivo nanomedicine. Hence, surface modifications of synthesized magnetizable nanoparticles (SPION, Mn-SPIO) were performed with oleic acid. There are numerous literatures available in which magnetizable nanoparticles are coated with oleic acid and dispersed in organic solvents. However, this limits their use in biomedical applications. This section details preparation of water based SPION, Mn-SPION and subsequent surface modification with oleic acid.

Superparamagnetic iron oxide nanoparticles (SPION) containing iron (II, III) oxide (Fe_3O_4) core

A modified version of co-precipitation technique used for the preparation of ferrofluids (Lopej, J. *et al.,* 2010, Mammani, J.B. *et al.,* 2013), reported in the literature, was used to prepare SPION containing iron (II, III) oxide core. SPIONs < 100 nm were prepared by precipitating a mixture of ferric (Fe^{3+}) and ferrous (Fe^{2+}) salts by ammonium hydroxide solution under carefully controlled experimental conditions. SPIONs were further stabilized by coating with oleic acid.

Novel superparamagnetic iron oxide nanoparticles containing mixed crystal manganese ferrite [$Mn_{0.1}Fe_{0.9}Fe_2O_4$] core (Mn-SPION)

In order to improve magnetic responsiveness, the magnetic core of iron (II, III) of SPION was replaced by manganese substituted mixed crystal ferrite [$Mn_{0.1}Fe_{0.9}Fe_2O_4$] core. SPION containing manganese substituted mixed crystal ferrite core was prepared by co-precipitation technique. Incorporation of manganous ion (Mn^{2+}) in crystal structure was achieved by simultaneous mixing of ferrous, ferric and manganous salts followed by precipitation with ammonium hydroxide solution under carefully controlled experimental conditions. Mn-SPIONs were further stabilized by coating with oleic acid.

Characterization of magnetic nanoparticles

Magnetic nanoparticles were characterized by X-ray diffraction (XRD) for structural analysis, dynamic light scattering (DLS) for particle size determination, scanning electron microscope (SEM) for morphology and fourier-transform infrared spectroscopy (FTIR) for chemical and structural analysis. Vibrating sample magnetometer (VSM) was used to study the magnetic properties.

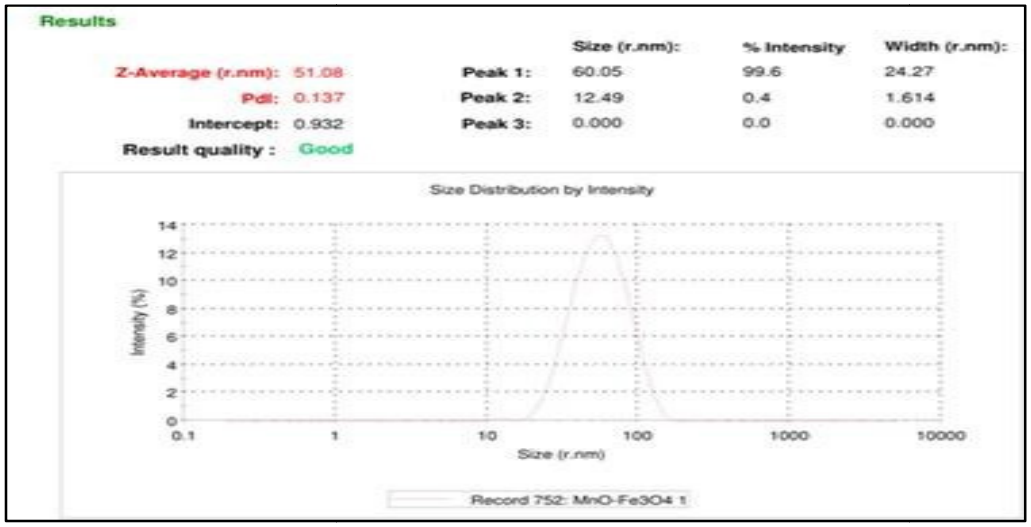

Figure 2.1

Particle size distribution of Mn-SPION

Average size of SPION and Mn-SPION (Figure 2.1) as determined by DLS were found to be less than 50 nm and 60 nm respectively. SEM images of SPION and Mn-SPION indicated formation of monodispersed particles of uniform size without any aggregation.

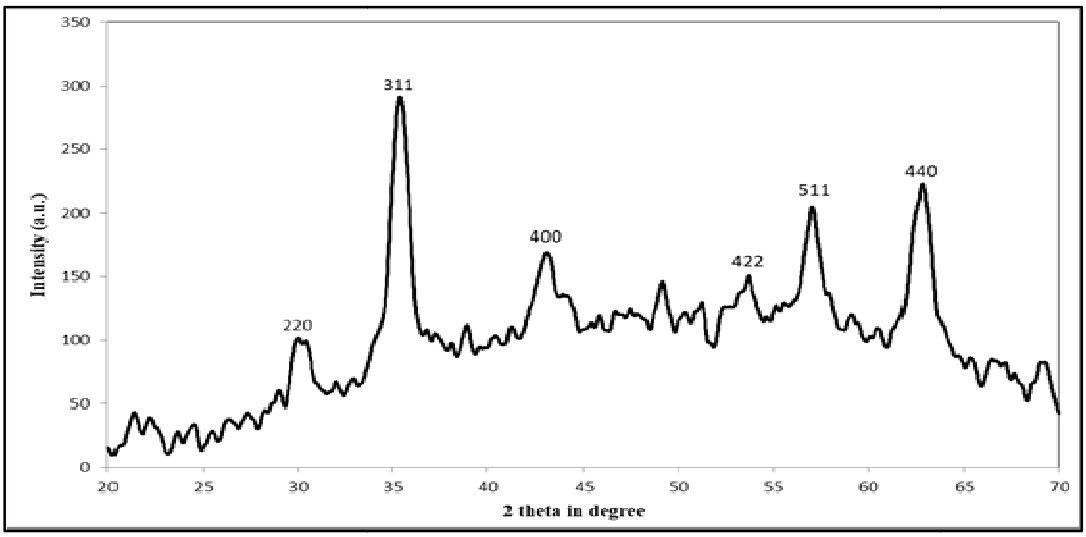

Figure 2.2

XRD Pattern of SPION

XRD analysis of SPION and Mn-SPION was carried out prior to oleic acid coating to confirm formation of iron (II, III) oxide and mixed crystal ferrite structure by indexing characteristic peaks, which were consistent with standard values in corresponding JCPDS

cards. XRD pattern of SPION is depicted in figure 2.2. The diffraction peaks of 2θ correspond to the [220], [311], [400], [422], [511], and [440] planes matched with JCPDS card number 85-1436 of magnetite. XRD pattern of Mn-SPION was similar.

Magnetic properties of magnetic nanoparticles were measured by vibrating sample magnetometer (VSM) at room temperature (RT) are shown in 2.3 and 2.4. In both cases, rapid saturation magnetization was observed. The saturation magnetization (Ms) of SPION and Mn-SPION are found to be 21.1emu/g and 16.5emu/g respectively. In addition, the particles exhibited negligible coercivity (Hc), absence of hysteresis loop in the M–H curve confirmed SPION and Mn-SPION are super paramagnetic in nature at RT.

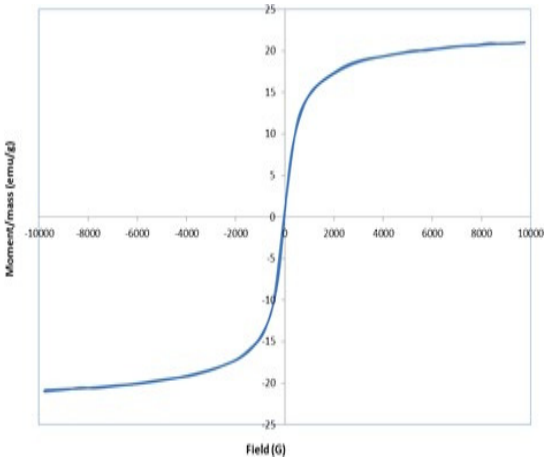

Figure 2.3
Hysteresis loop of SPION

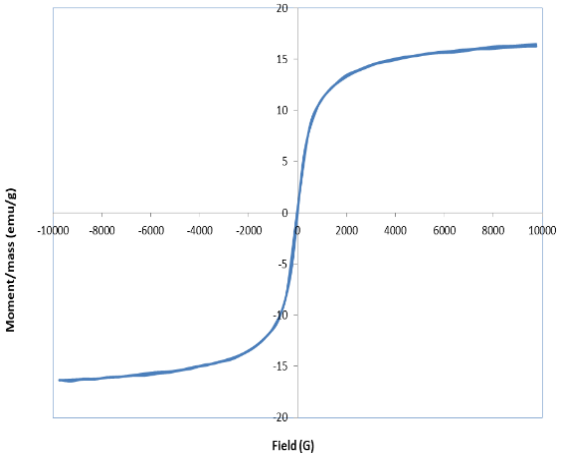

Figure 2.4
Hysteresis loop of Mn-SPION

Coating of magnetizable nanoparticles was confirmed by FTIR. Figure 2.5 depicts FTIR of Mn-SPION, pure oleic acid and Mn-SPION coated with oleic acid. The presence of -CH2 bonds (symmetric and asymmetric) and shift in -C=O stretching frequency to the lower value confirms the presence of oleic acid onto the surface ofMn-SPION.

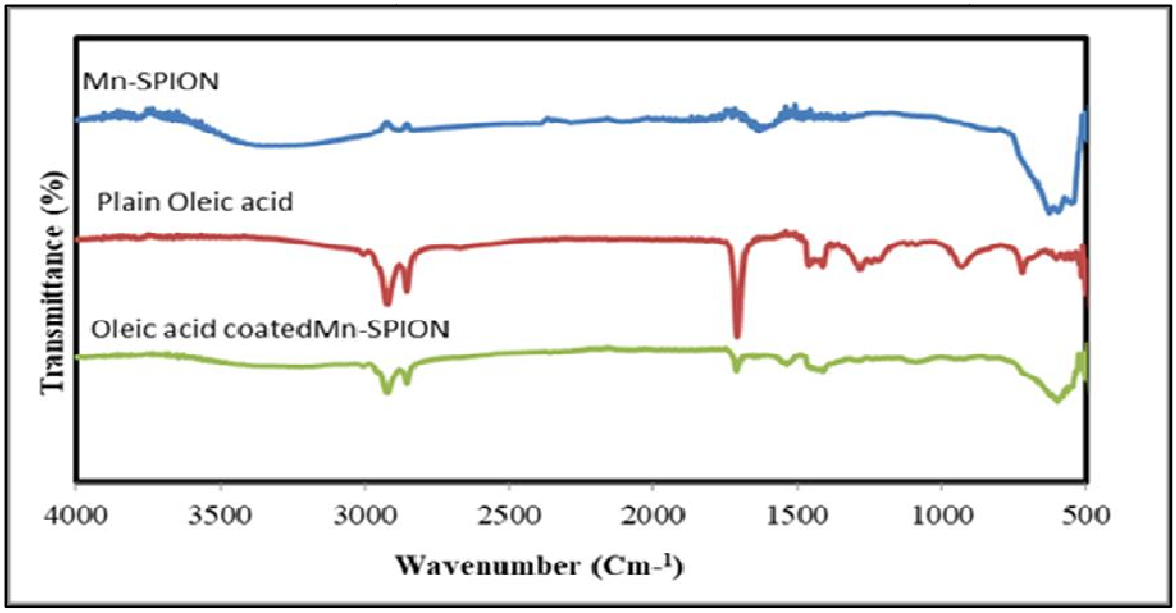

Figure 2.5
FTIR spectrum of (1) Mn-SPION (2) Plain oleic acid (3) Mn-SPION coated oleic acid

3 Development of magnetic nanoparticle based biomolecule probes for use in nuclear medicine

Two types of magnetizable particles (SPION and Mn-SPION) thus synthesized and characterized were used as basic building blocks for subsequent development of probes for use in nuclear medicine for both in-vivo and in-vitro applications.

Development and evaluation of magnetic nanoparticles for use in in-vivo nuclear medicine applications

In order to evaluate the utility of SPION and Mn-SPION in in-vivo nuclear medicine, especially for nuclear medicine imaging for the diagnosis of diseases, magnetic nanoparticles were labelled with ^{99m}Tc and ^{125}I. 2, 3 - dimercaptosuccinic acid (DMSA) and monoclonal antibody along with radioisotopes (^{99m}TC and ^{125}I) were used in designing different biomedical probes using magnetic nanoparticles.

Radioisotope labelling with ^{99m}Tc

Direct radiolabelling of nanoparticles coated with oleic acid: Both SPION and Mn-SPION coated with oleic acid were labelled with ^{99m}Tc. 1 mL (2.5 mg) of SPION in water for injection was passed through a 0.22-µm Millipore filter into a sterile vial. 200 µL (2 mg) of

$SnCl_2.2H_2O$ dissolved in water for injection was injected into the vial containing magnetic nanoparticles. Subsequently, 30 mCi (1.11 GBq) of ^{99m}Tc-pertechnetate ($^{99m}TcO_4^-$) eluted from a ^{99}Mo/^{99m}Tc generator supplied by BRIT (radioactive concentration 10 mCi/mL at the time of elution) was passed into the vial and the mixture was stirred and incubated for 10 min at RT. Thus, ^{99m}Tc labelled magnetic particles formed were stored at 4^0C till further use. Radioactivity associated with both particles and supernatant was counted. Labelling efficiency (LE) or radiochemical purity (RCP) was determined by instant thin layer chromatography (ITLC) and paper chromatography (PC).

Radiolabelling of nanoparticles functionalized with DMSA: Initially Mn-SPION coated with oleic acid were coated with a secondary layer of DMSA by the procedure described by L.N. Song *et al* (2017) and further labelled with ^{99m}Tc using similar procedure as described above. The pH of the reaction mixture was maintained below 4.0 during labelling reaction and the labelled product is stored at 4^0C till further use.

In-vitro stability studies of ^{99m}Tc labelled magnetic nanoparticles in serum: Labelling stability was tested in-vitro in the presence or absence of serum by determining the percentage of radioactivity associated with time. In order to determine the stability of the radiolabelled product in serum, immediately after labelling, 200 µL of labelled product was incubated with 1mL of pooled normal human serum and incubated at 37^0C. RCP at different interval of times were determined.

Biodistribution studies: Biodistribution studies of nanoparticles functionalized with DMSA were performed in Wistar rats. About 5 mCi (185 MBq) (approximately 0.2 mL) of the labelled product were injected through the tail vein of the animal. After 1 and 2 h of post injection, animals were sacrificed, relevant organs were removed, washed and radioactivity associated with the organs were counted. Finally, percentage of injected activity per organ (% IA/organ) was calculated using gamma counter calibrated for ^{99m}Tc.

The quality control (QC) procedure used to estimate the percentage of ^{99m}Tc labelled magnetic nanoparticles formed was ascending ITLC using silica gel (SG) coated plastic sheets. Acetone was used as mobile phase. Similarly, paper chromatography (PC) was also performed using Whatman chromatography strips and 85% methanol was used as a solvent. Radiocolloid formation was ruled out by measuring radioactivity associated with

magnetically separated labelled nanoparticles and the supernatant using a magnetic separator and the procedure described in user manual of the magnetic separator supplied by Ocean Nano Tech LLC, USA. Negligible radioactivity at supernatant was observed.

Labelling procedure for magnetic nanoparticles is optimized in order to get maximum RCP after studying the effect of stannous concentration, amount of radioactivity and reaction time. Amount of stannous chloride required is very important in the labelling process as higher amount results in formation of radio colloids, whereas lower amounts of stannous chloride results in poor labelling efficiency. Optimal amount of stannous chloride required for high labelling efficiency or RC purity (> 98%) was found to be 200 µg per 2.5 mg of nanoparticles. Incubation time of 10 min was found to be adequate. For optimizing above parameters at each time point, labelling efficiency or RCP was determined by ITLC. A typical radio paper chromatogram of reaction mixture is given in figure 3.1. In order to ensure the TcO_4^- in generator elute ITLC or PC of the generator $^{99}Mo/^{99m}Tc$ elute was performed along with every labeling procedure.

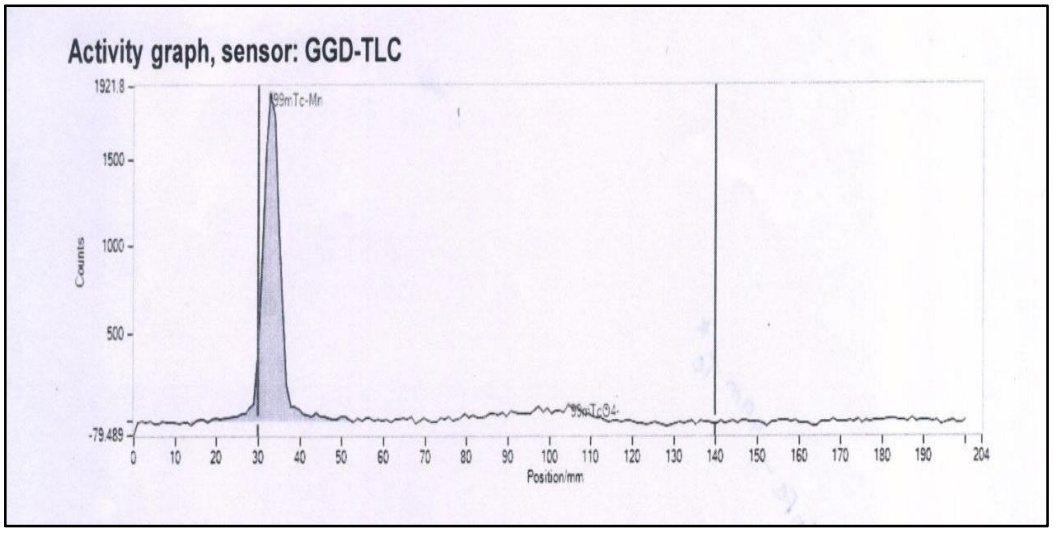

Figure 3.1

A typical radio paper chromatogram of Mn-SPION-DMSA - ^{99m}Tc

Labelling efficiency or RCP for radiolabelled products as determined by ITLC / PC immediately after preparation is given in table 3.1.

Table 3.1

Labelling efficiency with ^{99m}Tc labelled magnetic nanoparticles

Product	ITLC Solvent-Acetone		PC Solvent - 85% methanol	
	% RCP	% $^{99m}TcO_4$	% RCP	% $^{99m}TcO_4$
^{99m}Tc – SPION	99.17	0.83	98.10	1.9
^{99m}Tc Mn-SPION	99.23	0.77	98.25	1.75
^{99m}Tc Mn-SPION – DMSA	99.15	0.85	98.92	1.18

Radiolabelled preparations were checked for their in-vitro stability in human serum and in normal saline. These conditions were selected for stability study to mimic in-vivo environment of the body like serum proteins and physiological pH. There was no appreciable drop in RCP up to 6 hours which remained around 98 – 99%. However, there was reduction in RCP at 24 h (95% and 82% in saline and serum respectively). Biodistribution studies indicated ^{99m}Tc labelled Mn-SPION coated with DMSA were preferentially distributed in kidneys, liver and lungs. % IA/organ values post 1h of injection was 29.3, 13.3 and 8.2 for kidney, liver, and lungs respectively. In addition, about 2% IA/organ value for spleen was also observed. DMSA contains two sulfhydryl groups and its chelation property has been exploited in nuclear medicine. ^{99m}Tc labelled DMSA shows altered organ distribution depending on methods of preparation. At acidic pH (pH 2–4), as in the present case, DMSA chelates with technetium in lower oxidation (III) state and has binding affinity for the proximal tubular cells of the kidneys which explains higher uptake of ^{99m}Tc labelled Mn-SPION coated with DMSA in kidneys. Liver and spleen uptake of labelled product may be due to its colloidal nature.

Radioisotope labelling with ^{125}I

In order to demonstrate the utility of developed magnetic nanoparticles for antibody conjugation for potential biomedical applications, a monoclonal antibody was linked covalently to Mn-SPION. Monoclonal, anti-triiodothyronine (T3) antibody readily available at BRIT was used as a model antibody for this purpose. In the present study, monoclonal antibody was labelled with ^{125}I followed by its conjugation with magnetic nanoparticles.

Radioiodination of monoclonal antibody with ^{125}I: Radioiodination was carried out using chloramine T oxidation method followed by gel filtration using sephadex G-75. In order to achieve the specific activity of around 14 µCi/µg of ^{125}I radiolabelled monoclonal antibody, 20 µg of antibody was used along with 300 µCi of ^{125}I (supplied by Bhabha Atomic Research Centre, Mumbai, India) in the form of $Na^{125}I$. ^{125}I labelled and purified monoclonal antibody was stored at -20^0C. Radioiodination yield and radiochemical purity (RCP) were determined by paper chromatography (electrophoresis).

Conjugation of ^{125}I labelled monoclonal antibody to Mn-SPION: Briefly, to 2 mL (5 mg) of Mn-SPION coated with oleic acid, 1 mg of 1-ethyl-3-(3-dimethylaminopropyl) carbodiimide was added followed by 2 mL (50 µCi) ^{125}I labelled antibody and the reaction mixture was incubated overnight at room temperature. The resulting antibody magnetic nanoparticle conjugate was washed once with 0.05M phosphate buffer pH 7.4, using a powerful magnetic separator and using the procedure as described in the user manual of the magnetic separator supplied by Ocean Nano Tech LLC, USA.

During radioiodination of monoclonal antibody, incorporation of radioiodine into antibody was restricted maximum up to one atom of ^{125}I per antibody molecule corresponding to a specific activity of 15 µCi/µg. Specific activity and radiochemical purity of ^{125}I labelled monoclonal antibody was calculated using paper electrophoresis. Radioiodination yield of 83% was obtained corresponding to specific activity of 12.5 µCi/µg (0.86 of ^{125}I atom per antibody molecule). RCP of > 94% suggested the integrity of the radioiodinated product. Conjugation of labelled monoclonal antibody is confirmed by measuring radioactivity associated with magnetically separated conjugated nanoparticles and the supernatant over a period of time. Magnetically separated nanoparticles retained more than the 90% of the radioactivity.

Development and evaluation of magnetic nanoparticles for use in in-vitro nuclear medicine applications

This section details preparation of magnetizable cellulose containing manganese ferrite core followed by comprehensive, design, development, optimization and validation of RIA procedures for thyroid hormones, triiodothyronine (T3) and thyroxine (T4) based novel magnetizable cellulose particles prepared using Mn-SPION.

Preparation of magnetizable cellulose containing manganese ferrite core using superparamagnetic iron oxide nanoparticles containing mixed crystal manganese ferrite [$Mn_{0.1}Fe_{0.9}Fe_2O_4$] core (Mn-SPION)

Magnetizable cellulose particles containing manganese ferrite core were prepared by using a novel technique based on wet grinding of magnetic nanoparticles and cellulose in a stirred ball mill. Mn-SPION without oleic acid coating (5 g) and micro-crystalline cellulose powder (15 g) were mixed and added to distilled water (100 ml) containing 0.1ml Triton - X. The stirred ball mill was charged with 350 ml of grinding media (6 mm diameter, stainless steel balls) and 100 ml of above slurry (mixture of cellulose and iron oxide in water). The ball mill was run for 16 hours at 180 rpm at room temperature under continuous circulation of cooling water. Samples were drawn from the grinding pot at 4 h intervals for particle size determination. At the end of the grinding, the ground material along with the grinding medium was separated using a stainless steel strainer. The ground slurry of magnetizable cellulose containing manganese ferrite core was found to contain some agglomerate. These agglomerates of particles were broken by using ultrasonication (600 watt, 20 kHz) for 3 min.

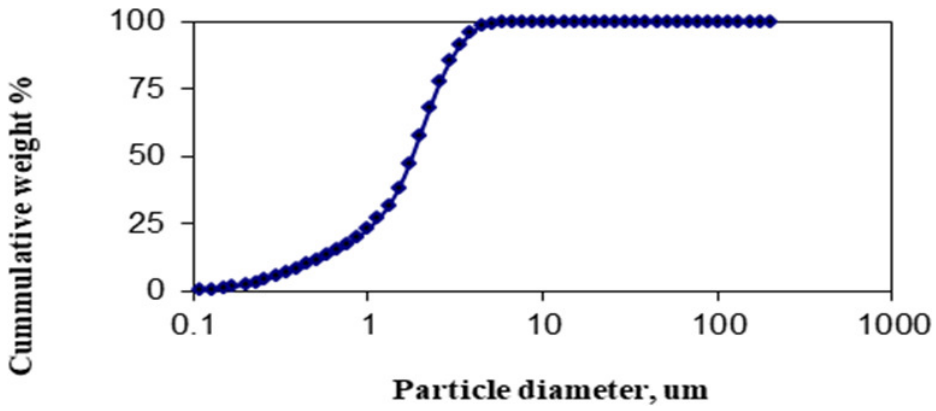

Figure 3.2

Particle size distribution of magnetizable cellulose containing manganese ferrite core

Particle size distribution as determine using Horiba-LA-500 laser diffraction particle size analyzer at the end of 16 h grinding is depicted in figure 3.2 and the average particle size of the magnetizable cellulose particles was found to be 1.81 µm with cut off size of 7.7 µm. Percentage on 2µm size particle was found to be 55.4 and the specific surface area as

calculated by the same equipment was found to be 58123 m^2/cm^3. By this new, simple and easy to adopt one-step wet grinding technique, it has been possible to achieve a firm physical binding between magnetic nanoparticles and cellulose and also to reduce the size of the particles below 2µm.

Immobilization of antibodies on magnetizable cellulose particles containing manganese ferrite core

Immobilization of the antibody on magnetizable cellulose containing manganese ferrite core was carried out by activating the -OH groups present on the cellulose of these particles with 1, 1'- carbonyldiimidazole, followed by the addition of antibody. Thus, a firm and efficient covalent bonding is achieved between the $-NH_2$ groups present in the antibody and -OH groups available on the particles. This resulted in more than 70% uptake of the antibody (monitored spectrophotometrically) and the immunosorbent formed was found to be stable at least up to two years when store at 4^0C. In all the immobilization procedures, various factors such as quantity of the particles / antibody required, time required for the immobilization, non-specific uptake of the particles etc., have been studied, in order to achieve the optimal coupling of antibodies to the particles.

Development of Radioimmunoassay Procedures for Thyroid Hormones - Triiodothyronine (T3) and Thyroxine (T4) using magnetizable cellulose particles containing manganese ferrite core

As thyroid hormones (T3 and T4) are major biomarkers for the detection and management of thyroid diseases, RIA procedures for the serum measurements of thyroid hormones, triiodothyronine (T3) and thyroxine (T4) were designed, developed, and validated using antibody conjugated magnetizable cellulose particles containing manganese ferrite core are detailed here. Following RIA kit reagents were prepared and characterized for the development of RIA kit formulations for T3 and T4:

^{125}I labelled antigen (tracer): For the preparation of T3 tracer, T2 (diiodothyronine) was radiolabelled with ^{125}I using chloramine-T oxidation method and purified by gel permeation chromatography. The specific activity of the radiolabelled T3 was maintained around 3000 µCi/µg, which is about one atom of ^{125}I per molecule of T3. On the day of preparation, the count rate was maintained between 60,000-70,000 cpm/tube (at 80% counting efficiency). For the preparation of T4 tracer, commercial T4 was radiolabelled with ^{125}I. The specific

activity of the radiolabelled antibody was maintained at 800 µCi/µg, on the day of preparation, the count rate was maintained between 80,000-90,000 cpm/tube. Both the radiolabelled products were lyophilized and stored at 4^0C.

Standards (calibrators): For T3 RIA, a set of 6 standards (0, 0.3, 0.6, 1.2, 2.4 and 4.8 ng/mL) were prepared using bovine serum matrix depleted of T3 by charcoal treatment. Similarly, for T4 RIA, a set of 6 standards (0, 15, 30, 60, 120 and 240 ng/mL) were prepared in bovine serum matrix depleted of T4 by charcoal treatment. These standards prepared in bovine serum matrix with preservative sodium azide were stored frozen at - 20˚C.

Kit controls: Two T3 controls at different levels (~1.2 ng/mL and 2.2 ng/mL) were prepared by spiking calculated amount of T3 in human serum containing sodium azide, aliquoted and lyophilized. Two T4 controls at different levels (~ 60 ng/mL and 120 ng/mL) were prepared by spiking calculated amount of T4 in human serum containing sodium azide, aliquoted and lyophilized.

Assay buffer: 0.014 M tris buffer, pH 7.4, containing 0.1% sodium azide and 0.2% BSA was used as assay buffer for both, T3 and T4 RIA.

Wash Solution: Phosphate buffer saline containing 0.1% sodium azide, 0.2% BSA and 0.1% Tween – 20 was used as wash solution for both T3 and T4 RIA.

Kit antibody – magnetic particle suspension: Antibody coupled to magnetizable cellulose containing manganese ferrite core for T3 RIA was prepared by using commercial rabbit, anti-T3 polyclonal antibody (screened and identified specifically for this purpose and previously characterized) at 1:22,000 dilution was used. Similarly, for T4 RIA in-house rabbit, anti-T4 polyclonal antibody at 1:1000 dilution was used. Conjugation (functionalization or coupling) of antibody to magnetizable cellulose particles was carried out using optimized CDI activation method described earlier. Kit antibody – magnetic particle suspension was stored at 4˚C.

Knowing the affinity constant of an antibody allows judicious selection of antibody for a specific purpose. Purified antiserum with high affinity constant is desirable in the development of solid phase immunoassays as there will be a significant reduction in the

affinities of the antibodies upon linkage to the solid supports including magnetizable particles. Hence, affinity constants of antibodies were determined by Scatchard plots for raw, salt precipitated / purified and magnetizable cellulose containing manganese ferrite core bound antibodies using their optimal dilutions. Results are summarized in table3.2.

Table 3.2

Affinity constants of raw, purified and solid phase antibodies

Antibody (Ab)	Affinity Constant (litres /mole)		
	Raw antibody	Purified antibody	Solid phase or mag cellulose bound antibody
Anti-T4 Ab	2.00×10^{11}	3.90×10^{11}	1.53×10^{11}
Anti-T3 Ab	1.60×10^{12}	1.55×10^{12}	1.93×10^{10}

As expected, reduction in affinity constant (K) of antibody was observed after conjugation to magnetic particles. As the detection limit or sensitivity of RIA is mainly governed by the affinity, and the loss of sensitivity on the account of conjugation of antibody to solid supports (plastic tubes / beads, latex or magnetic particles) can be compensated partly by using solid supports with minimum NSB. Improved magnetic responsiveness of magnetizable cellulose particles containing manganese ferrite core offered low non-specific binding (NSB).

RIA procedures for T3 and T4 were standardized after optimization of standard assay parameters such as incubation time, temperature, amount of tracer, sample volume and titre of antibody linked magnetizable particles required etc. In addition, stability of the individual kit components such as tracer, standards, antibody-magnetic particles suspension as well as that of assembled kits were also studied.

Optimized assay protocol T3 RIA: Add 50 µL each of standard / sample, 100 µL anti-T3 antibody coupled magnetizable cellulose containing manganese ferrite core suspension and 100 µL of I-125 labelled T3 to assay tubes and incubate for 3 h at RT with stirring. At the end of the incubation, add 1 mL of wash solution to each of the test tubes and separate

magnetizable cellulose particles using a magnetic separator. Measure the activity associated with magnetizable cellulose particles for 1 min using a gamma counter calibrated for I-125. Construct a standard curve by plotting CPM (Y-axis) versus the standard concentration (X-axis) on a logit-log paper. Read the concentrations of T3 from the standard curve.

Optimized assay protocol T4 RIA: Add 25 µL each of standard / sample, 100 µL anti-T4 antibody coupled magnetizable cellulose containing manganese ferrite core suspension and 100 µL of I-125 labelled T4 to assay tubes and incubate for 2h at RT. At the end of the incubation, add 1 mL of wash solution to each of the test tubes and separate magnetizable cellulose particles using a magnetic separator. Measure the activity associated with magnetizable cellulose particles for 1 min using a gamma counter calibrated for I-125. Construct a standard curve by plotting CPM (Y-axis) versus the standard concentration (X-axis) on a semi-log paper. Read the concentrations of T4 from the standard curve.

Validation of RIA procedures for Thyroid Hormones - Triiodothyronine (T3) and Thyroxine (T4) using magnetizable cellulose particles containing manganese ferrite core

Validation of the developed RIA procedures and subsequent kit formulations were carried out using statistical methods applicable for immunoassays.

Sensitivity: For the determination of the sensitivity, standard curves were set up and plotted as per the optimized RIA protocol, but zero standard was set up in ten replicates. For zero standard concentration, mean and the standard deviation of the replicate's CPM were calculated. The antigen concentration corresponding to the mean minus two standard deviations of the zero standard is considered to represent the sensitivity.

Specificity: The specificity of anti T3 serum, was established by determining its cross reaction with the structurally similar and most probable cross reacting analogue, T4 present in the human serum at much higher concentration. Similarly, the specificity of all anti T4 sera were established by determining their cross reaction T3 present in relatively much lower concentration.

Assay variations: The intra-assay variation was determined by analyzing 2 serum samples

15 times in the same assay while the inter-assay variation was determined by analyzing the same two serum samples in 10 different assays (in duplicate) run over a period of a time (one month).

Recovery and linearity of dilution studies: For estimation of recovery, serum sample containing T3 or T4 were spiked with a known amount of T3 or T4 standards. The native sample and the spiked sample were analyzed in the same assay. For linearity of dilution studies, samples containing T3 and T4 were diluted 2-fold, 4-fold and 8-fold with zero standard. Both native samples as well as diluted samples were analyzed in the same assay.

Sample drift studies: Two serum samples were repeatedly analyzed in the same assay at different intervals of time using optimized assay protocol.

Stability studies: Stability of each RIA reagents ^{125}I labelled antigen (tracer), Standards (calibrators), kit controls and kit antibody) were studied over a period of time.

Procedures for handling I-125 and radioactive waste disposal: Guidelines laid done by Atomic Energy Regulatory Board, India were strictly followed while handling of I-125, including procurement, storage, radioiodination, setting up of RIA and disposal of radioactive waste.

Analytical performance characteristics of T3 and T4 RIA kit formulations are summarized in table 3.3 and all the parameters listed are within the acceptable limits applicable for immunoassay kit formulations. In addition, around 100 clinical samples from hypo, hyper and euthyroid patients were analyzed using developed kit.

T3 and T4 values obtained were compared with those values obtained by an established commercial T3 and T4 RIA kits respectively. Both the methods gave similar sample values with r = 0.98 (n= 92) in the case of T3 and r = 0.97 (n=95) in the case of T4 RIA.

Table 3.3
Analytical performance characteristics of developed kit formulations

Sr. No.	Parameters	T3 RIA	T4 RIA
1.	Standard / Sample volume	50 µL	25 µL
2	Standard range	0.3 – 4.8 ng / mL	15 – 240 ng/mL
3.	Sensitivity	0.18 ng/mL	8 ng / mL
4.	Incubation	3 h at RT (stirring)	2 h at RT
5.	Specificity	100 % with T3 0.033% with T4	100 % with T4 1.05 % with T3
6.	Precision 1) Intra-assay variations 2) Inter-assay variations	 4.8 % 9.8 %	 3.9 % 7.1 %
7.	Recovery	93 - 108 %	94 – 106 %
8.	Dilution linearity	90 - 111%	91 – 109 %
9.	Assay drift	Not observed up to 20 min	Not observed up to 20 min
10.	Normal range Hypothyroid Euthyroid (normal) Hyper thyroid	 < 0.7 ng/mL 0.7 – 2.1 ng/mL > 2.1 ng/mL	 < 55 ng/mL 55– 135 ng/mL > 135 ng/mL
11.	Stability of reagents Tracer Standards Kit controls Kit antibody	 60 days 1 year 2 year 1 year	 60 days 1 year 2 year 1 year

4. Summary and conclusions

Synthesis and characterization of versatile magnetizable nanoparticles

Two types of magnetizable particles below 60 nm of average particle size were prepared by co-precipitation technique under controlled experimental conditions followed by biocompatible surface coating with oleic acid in an aqueous medium: Superparamagnetic iron oxide particles (SPION) and novel superparamagnetic iron oxide particles containing manganese ferrite ($Mn_{0.1}Fe_{0.9}Fe_2O_4$) core (Mn-SPION). Manganese substitution in iron oxide core leads to increase in the magnetic responsiveness of nanoparticles. These particles can be used as basic building blocks in the architecture of nanoparticle based biomedical probes.

Development of superparamagnetic nanoparticle based biomolecule probe

Development and evaluation of superparamagnetic nanoparticle based biomolecule probes by combining magnetic properties with radioisotopes for the potential use in nuclear medicine applications was carried out. Radiolabelling procedures with ^{99m}Tc and ^{125I} of nanoparticles were standardized.

For in-vivo nuclear medicine applications: ^{99m}Tc - DMSA (III) - Mn-SPION probe for potential multimodal nuclear medicine imaging based on SPECT-MRI was developed and evaluated for RCP, in-vitro serum stability and in-vivo biodistribution. In addition, stable ^{125}I labelled monoclonal antibody – Mn-SPION prepared demonstrated the amenability of synthesized nanoparticles for functionalization with radiolabelled monoclonal antibodies.

Although the present study had demonstrated the designing of flexible SPION-biomolecule interface of different configurations in general, it is important that SPION based biomolecule probes if used *in-vivo* must also have a surface coating which is also eventually biodegradable, biocompatible and has low or non-cytotoxicity with cells. There are number of publications reporting successful in-vivo applications of SPION coated with oleic acid such as magnetic resonance imaging, targeted delivery of drugs or genes, hyperthermia etc. Future work would be carried out to access the in-vivo toxicity of SPION based biomolecule probes designed for the specific purpose.

For in-vitro nuclear medicine applications: Magnetizable cellulose containing manganese ferrite core was prepared by entrapping nanoparticles in cellulose matrix for use in in-vitro nuclear medicine applications such as RIA, IRMA, cell separation, affinity chromatography etc. Wet grinding technique adopted here can control the particle size as per the requirement.

Magnetizable cellulose particles containing manganese ferrite core thus prepared is a synergistic composition and so far not reported in the literature.

Development of RIA for thyroid hormones for detection and management of thyroid diseases

RIA procedures followed by kit formulations were designed, developed and validated for the serum measurements of thyroid hormones, triiodothyronine (T3) and thyroxine (T4) using antibody conjugated magnetizable cellulose particles containing manganese ferrite core. Large scale production of RIA kits is possible. Production manual as per ISO 9001:2015 & 13485:2012 were also prepared.

5. References

1. Aryal, S., Hu, C. M. J., Fu, V., & Zhang, L. (2012). Nanoparticle drug delivery enhances the cytotoxicity of hydrophobic–hydrophilic drug conjugates. *Journal of Materials Chemistry*, *22*(3), 994-999.

2. Assadi, M., Afrasiabi, K., Nabipour, I., & Seyedabadi, M. (2011). Nanotechnology and nuclear medicine; research and preclinical applications. *Hellenic journal of nuclear medicine*, *14*(2), 149.

3. Atomic, E. R. B. (2011). *Classification of radioactive waste* (No. AERB/NRF/SG/RW--1). Atomic Energy Regulatory Board.

4. Beeran, A. E., Nazeer, S. S., Fernandez, F. B., Muvvala, K. S., Wunderlich, W., Anil, S., & Varma, P. H. (2015). An aqueous method for the controlled manganese (Mn 2+) substitution in superparamagnetic iron oxide nanoparticles for contrast enhancement in MRI. *Physical Chemistry Chemical Physics*, *17*(6), 4609-4619.

5. Bhattacharyya, D., Singh, S., Satnalika, N., Khandelwal, A., & Jeon, S. H. (2009). Nanotechnology, big things from a tiny world: a review. *International Journal of u- and e-Service, Science and Technology*, *2*(3), 29-38.

6. Fu, C. M., Wang, Y. F., Chao, Y. C., Hung, S. H., & Yang, M. D. (2004). Directly labeling ferrite nanoparticles with Tc-99m radioisotope for diagnostic applications. *IEEE transactions on magnetics*, *40*(4), 3003-3005.

7. Gelperina, S., Kisich, K., Iseman, M. D., & Heifets, L. (2005). The potential advantages of nanoparticle drug delivery systems in chemotherapy of tuberculosis. *American journal of respiratory and critical care medicine*, *172*(12), 1487-1490.

8. GUIDE, A. S. (2015). RADIOISOTOPE HANDLING FACILITIES.

9. Hong, H., Zhang, Y., Sun, J., & Cai, W. (2009). Molecular imaging and therapy of cancer with radiolabeled nanoparticles. *Nano today*, *4*(5), 399-413.

10. Hutton, B. F., Occhipinti, M., Kuehne, A., Máthé, D., Kovács, N., Waiczies, H., & Short, S. C. (2018). Development of clinical simultaneous SPECT/MRI. *The British journal of radiology*, *91*(1081), 20160690.

11. Justin, C., Philip, S. A., & Samrot, A. V. (2017). Synthesis and characterization of superparamagnetic iron-oxide nanoparticles (SPIONs) and utilization of SPIONs in X-ray imaging. *Applied Nanoscience*, *7*(7), 463-475.

12. Kadwad, V., Jyotsna, N., Sivaprasad, N., & Sinha, P. (1996). A method for preparation of magnetizable cellulose and its application in radioimmunoassays for T3 and T 41. *Journal of radioanalytical and nuclear chemistry*, *210*(1), 27-33.

13. Kanagesan, S., Aziz, S. B. A., Hashim, M., Ismail, I., Tamilselvan, S., Alitheen, N. B. B. M., & Purna Chandra Rao, B. (2016). Synthesis, characterization and in vitro evaluation of manganese ferrite (MnFe2O4) nanoparticles for their biocompatibility with murine breast cancer cells (4T1). *Molecules*, *21*(3), 312.

14. Kohler, N., Sun, C., Wang, J., & Zhang, M. (2005). Methotrexate-modified superparamagnetic nanoparticles and their intracellular uptake into human cancer cells. *Langmuir*, *21*(19), 8858-8864.

15. Kolhatkar, A. G., Jamison, A. C., Litvinov, D., Willson, R. C., & Lee, T. R. (2013). Tuning the magnetic properties of nanoparticles. *International journal of molecular sciences*, *14*(8), 15977-16009.

16. Kong, D., & Wilson, L. D. (2018). Structural study of cellulose-iron oxide composite materials. *Journal of Materials Science and Chemical Engineering*, *6*(4), 65-77.

17. Krishnan, K. M. (2010). Biomedical nanomagnetics: a spin through possibilities in imaging, diagnostics, and therapy. *IEEE transactions on magnetics*, *46*(7), 2523-2558.

18. Kudr, J., Haddad, Y., Richtera, L., Heger, Z., Cernak, M., Adam, V., & Zitka, O. (2017). Magnetic nanoparticles: From design and synthesis to real world applications. *Nanomaterials*, *7*(9), 243.

19. Leary, S. P., Liu, C. Y., Yu, C., & Apuzzo, M. L. (2005). Toward the emergence of nanoneurosurgery: Part I—Progress in nanoscience, nanotechnology, and the comprehension of events in the mesoscale realm. *Neurosurgery*, *57*(4), 606-634.

20. Lee, H. Y., Li, Z., Chen, K., Hsu, A. R., Xu, C., Xie, J., & Chen, X. (2008). PET/MRI dual-modality tumor imaging using arginine-glycine-aspartic (RGD)–conjugated radiolabeled iron oxide nanoparticles. *Journal of Nuclear Medicine*, *49*(8), 1371-1379.

21. Leinonen, A., & Kivisaari, S. (2010). *Nanotechnology perceptions: Literature review on media coverage, public opinion and NGO perspectives*. VTT Technical Research Centre of Finland.

22. Li, Q., Kartikowati, C. W., Horie, S., Ogi, T., Iwaki, T., & Okuyama, K. (2017). Correlation between particle size/domain structure and magnetic properties of highly crystalline Fe 3 O 4 nanoparticles. *Scientific reports*, *7*(1), 1-7.

23. Lodhia, J., Mandarano, G., Ferris, N. J., Eu, P., & Cowell, S. F. (2010). Development and use of iron oxide nanoparticles (Part 1): Synthesis of iron oxide nanoparticles for MRI. *Biomedical imaging and intervention journal*, *6*(2), e12.

24. Lopez, J. A., González, F., Bonilla, F. A., Zambrano, G., & Gómez, M. E. (2010). SYNTHESIS AND CHARACTERIZATION OF Fe3O4 MAGNETIC NANOFLUID. *RevistaLatinoamericana de Metalurgia y Materiales*, *30*(1), 60-66.

25. Madru, R., Kjellman, P., Olsson, F., Wingårdh, K., Ingvar, C., Ståhlberg, F., ...& Strand, S. E. (2012). 99mTc-labeled superparamagnetic iron oxide nanoparticles for multimodality SPECT/MRI of sentinel lymph nodes. *Journal of Nuclear Medicine*, *53*(3), 459-463.

26. Mamani, J. B., Costa-Filho, A. J., Cornejo, D. R., Vieira, E. D., & Gamarra, L. F. (2013). Synthesis and characterization of magnetite nanoparticles coated with lauric acid. *Materials Characterization*, *81*, 28-36.

27. Mamani, J. B., Gamarra, L. F., & Brito, G. E. D. S. (2014). Synthesis and characterization of Fe3O4 nanoparticles with perspectives in biomedical applications. *Materials Research*, *17*(3), 542-549.

28. Mandarano, G., Lodhia, J., Eu, P., Ferris, N. J., Davidson, R., & Cowell, S. F. (2010). Development and use of iron oxide nanoparticles (Part 2): The application of iron oxide contrast agents in MRI. *Biomedical Imaging and Intervention Journal*, *6*(2), e13.

29. Mirković, M., Radović, M., Stanković, D., Milanović, Z.,Janković, D., Matović, M., & Vranješ-Đurić, S. (2019). 99mTc–bisphosphonate–coated magnetic nanoparticles as potential theranostic nanoagent. *Materials Science and Engineering: C*, *102*, 124-133.

30. Misri, R., Saatchi, K., & Häfeli, U. O. (2012). Nanoprobes for hybrid SPECT/MR molecular imaging. *Nanomedicine*, *7*(5), 719-733.

31. Nikitin, P. I., Vetoshko, P. M., & Ksenevich, T. I. (2007). Magnetic immunoassays. *Sensor Letters*, *5*(1), 296-299.

32. Patil, R. M., Shete, P. B., Thorat, N. D., Otari, S. V., Barick, K. C., Prasad, A.,& Pawar, S. H. (2014). Non-aqueous to aqueous phase transfer of oleic acid coated iron oxide nanoparticles for hyperthermia application. *RSC advances*, *4*(9), 4515-4522.

33. Pellico, J., Llop, J., Fernández-Barahona, I., Bhavesh, R., Ruiz-Cabello, J., & Herranz, F. (2017). Iron oxide nanoradiomaterials: combining nanoscale properties with radioisotopes for enhanced molecular imaging. *Contrast media & molecular imaging*, *2017*.

34. Pham, T. N., Lengkeek, N. A., Greguric, I., Kim, B. J., Pellegrini, P. A., Bickley, S. A., Tanudji, M. R., Jones, S. K., Hawkett, B. S., & Pham, B. T. (2017). Tunable and noncytotoxic PET/SPECT-MRI multimodality imaging probes using colloidally stable ligand-free superparamagnetic iron oxide nanoparticles. *International journal of nanomedicine*, *12*, 899–909.

35. Prodan, A. M., Iconaru, S. L., Ciobanu, C. S., Chifiriuc, M. C., Stoicea, M., & Predoi, D. (2013). Iron oxide magnetic nanoparticles: characterization and toxicity evaluation by in vitro and in vivo assays. *journal of Nanomaterials*, *2013*, 1-10.

36. Psimadas, D., Bouziotis, P., Georgoulias, P., Valotassiou, V., Tsotakos, T., & Loudos, G. (2013). Radiolabeling approaches of nanoparticles with 99mTc. *Contrast media & molecular imaging*, *8*(4), 333-339.

37. Rasmi, R. R., Shenoy, K. B., Kadwad, V. B., Sarnaik, J., &Somashekarappa, H. M. (2015). Application of novel magnetizable cellulose particles in the development of immunoradiometric assay for C-peptide. *Journal of Radioanalytical and Nuclear Chemistry*, *304*(3), 1115-1122.

38. Sahoo, B., Sahu, S. K., Nayak, S., Dhara, D., & Pramanik, P. (2012). Fabrication of magnetic mesoporous manganese ferrite nanocomposites as efficient catalyst for degradation of dye pollutants. *Catalysis Science & Technology*, *2*(7), 1367-1374.

39. Sarkar, Z. K., & Sarkar, F. K. (2011). Synthesis and magnetic properties investigations of Fe3O4 nanoparticles. *vol*, *7*, 197-200.

40. Sintya, E. (2018). Synthesis of 99m tc (V)-DMSA and radiolabelling of SPIO nanoparticles. *MS&E*, *434*(1), 012152.

41. Soares, P. I., Laia, C. A., Carvalho, A., Pereira, L. C., Coutinho, J. T., Ferreira, I. M., ... & Borges, J. P. (2016). Iron oxide nanoparticles stabilized with a bilayer of oleic acid for magnetic hyperthermia and MRI applications. *Applied Surface Science*, *383*, 240-247.

42. Song, L. N., Gu, N., & Zhang, Y. (2017, January). A moderate method for preparation DMSA coated Fe3O4 nanoparticles. In *IOP Conference Series: Materials Science and Engineering* (Vol. 164, No. 1, p. 012026). IOP Publishing.

43. Surowiec, Z., Budzyński, M., Durak, K., & Czernel, G. (2017). Synthesis and characterization of iron oxide magnetic nanoparticles. *Nukleonika*, *62*(2), 73-77.

44. Tharani, K., & Nehru, L. C. (2015). Synthesis and characterization of iron oxide nanoparticle by precipitation method. *Int J Adv Res PhysSci*, *2*, 47-50.

45. Tsoukalas, C., Psimadas, D., Kastis, G. A., Koutoulidis, V., Harris, A. L., Paravatou-Petsotas, M., & Bouziotis, P. (2018). A novel metal-based imaging probe for targeted dual-modality SPECT/MR imaging of angiogenesis. *Frontiers in chemistry*, *6*, 224.

46. Tsui, B., Xu, J., Rittenbach, A., El-Sharkawy, A. M., Edelstein, W., Parnham, K., & Hugg, J. (2013). A completed SPECT/MR insert for simultaneous SPECT/MR imaging of small animals. *Journal of Nuclear Medicine*, *54*(supplement 2), 595-595.

47. Ünak, P. (2008). Imaging and therapy with radionuclide labeled magnetic nanoparticles. *Brazilian Archives of Biology and Technology*, *51*(spe), 31-37.

48. Unterweger, H., Dézsi, L., Matuszak, J., Janko, C., Poettler, M., Jordan, J., & Alexiou, C. (2018). Dextran-coated superparamagnetic iron oxide nanoparticles for magnetic resonance imaging: Evaluation of size-dependent imaging properties, storage stability and safety. *International journal of nanomedicine*, *13*, 1899.

49. Wierzbinski, K. R., Szymanski, T., Rozwadowska, N., Rybka, J. D., Zimna, A., Zalewski, T.,& Fiedorowicz, M. (2018). Potential use of superparamagnetic iron oxide nanoparticles for in vitro and in vivo bioimaging of human myoblasts. *Scientific reports*, *8*(1), 1-17.

50. Xu, H., Aguilar, Z. P., Yang, L., Kuang, M., Duan, H., Xiong, Y., ... & Wang, A. (2011). Antibody conjugated magnetic iron oxide nanoparticles for cancer cell separation in fresh whole blood. *Biomaterials*, *32*(36), 9758-9765.

51. Yang, C. T., Ghosh, K. K., Padmanabhan, P., Langer, O., Liu, J., Eng, D. N. C., ... & Gulyás, B. (2018). PET-MR and SPECT-MR multimodality probes: Development and challenges. *Theranostics*, *8*(22), 6210.

52. Yang, L. X., Wang, F., Meng, Y. F., Tang, Q. H., & Liu, Z. Q. (2013). Fabrication and characterization of manganese ferrite nanospheres as a magnetic adsorbent of chromium. *Journal of Nanomaterials*, *2013*.

53. Zipare, K., Dhumal, J., Bandgar, S., Mathe, V., & Shahane, G. (2015). Superparamagnetic manganese ferrite nanoparticles: synthesis and magnetic properties. *Journal of Nanoscience and Nanoengineering*, *1*(3), 178-182.

(Shripriya Purohit) (Dr. Vijay B. Kadwad)

Research Student **Research Supervisor**

Publications:

1. Shripriya Purohit, Archana Ghodke, Vijay Kadwad, K. Bhaskar Shenoy. 2019. Synthesis of Super paramagnetic iron oxide nanoparticles containing manganese ferrite core for radioisotope based biomedical applications, *Indian J Nucl Med* (IJNM)., Vol.34(5):1-109.
   (Presented a poster on the topic entitled, "Synthesis of Super paramagnetic iron oxide nanoparticles containing manganese ferrite core for radioisotope based biomedical applications" in the National Annual Conference of Society of Nuclear Medicine, India (SNMICON 2019) organized by Department of Nuclear Medicine & Molecular Imaging, Tata Memorial Hospital, Mumbai on 12-15 December2019)

2. Shripriya Purohit, V.B. Kadwad, S.S. Sachdev, K.B. Shenoy, H.M. Somashekarappa. 2018. Radioimmunoassay (RIA) Procedures for Triiodothyronine (T3) and Thyroxine (T4) Based on Novel Micro-magnetizable Cellulose Particles Containing Manganese Ferrite Core, Proceedings: NAARRI International Conference on Advanced Applications of RadiationTechnology.1-133.
   (Presented a poster on the topic entitled, "Radioimmunoassay (RIA) Procedures for Triiodothyronine (T3) and Thyroxine (T4) Based on Novel Micro-magnetizable Cellulose Particles Containing Manganese Ferrite Core" on 05-07 March 2018 in the NAARRI International Conference on "Advanced Applications Of Radiation Technology" (NICSTAR-2018) organized by National Association for Application of Radioisotopes and Radiation in Industry (NAARRI),Mumbai)

3. Shripriya Purohit, Vijay Kadwad, Jayula Sarnaik, Rani Gnanasekar, Shalaka Paradkar and Satbir Singh Sachdev. 2015. Studies on Antibody Affinity Constants on Operational Aspects of Liquid Phase and Solid Phase RIA Development, *Indian J Nucl Med* (IJNM)., Vol.30 (5):1-72.

4. Jayula Sarnaik, Shripriya Purohit, Vijay Kadwad, Shalaka Paradkar, Rani Gnanasekar, Satbir Singh Sachdev. 2016. Radioimmunoassay of Triiodothyronine in Rat Serum, Journal of Radiation and Cancer Research, vol.7 (5):1-56.

5. Shripriya K. Purohit, Archana S. Ghodke, Vijay B. Kadwad & Shenoy K.B. 2022. A Method of Preparation for Superparamagnetic Iron Oxide Nanoparticles Containing Mixed Crystal Manganese Ferrite Core (Mn-SPION) for the Development of Biomolecule Probes for Detection and Management of Diseases. Proceedings: International conference on Advances in Biosciences and Biotechnology 2022, VSRD INTERNATIONAL JOURNAL OF BIO-TECHNOLOGY AND PHARMACEUTICAL SCIENCES, ISSN:2278-9197 [Special Issue Vol. XI, Jan 2022]:1-248.

   (Orally presented a paper entitled "A Method of Preparation for Superparamagnetic Iron Oxide Nanoparticles Containing Mixed Crystal Manganese Ferrite Core (Mn-SPION) for the Development of Biomolecule Probes for Detection and Management of Diseases" on 20-22 January 2022 in the online International conference on Advances in Biosciences and Biotechnology (ICABB-2022) organized by Department of Biotechnology, Jaypee Institute of Information and Technology, Noida, Uttar Pradesh, India.